Eur. Phys. J. C manuscript No.
(will be inserted by the editor)

Physics potential for the measurement of the H→ZZ decay at the CEPC

Yanxi Gu[1], Min Zhong[1], Ryuta Kiuchi[2], Shih-Chieh Hsu[a,3], Xin Shi[b,2], Kaili Zhang[2]

[1]Department of Modern Physics, University of Science and Technology of China, Hefei, China
[2]Institude of High Energy Physics, Chinese Academy of Science, Beijing 100049, China
[3]Department of Physics, University of Washington, Seattle 98195-1560, USA

Received: date / Accepted: date

Abstract The precision of the yield measurement of the Higgs boson decaying into two Z bosons process at the Circular Electrion-Positron Collider (CEPC) is evaluated. Including the recoil Z boson associated with the Higgs production (Higgsstrahlung) total three Z bosons involves for this channel, from which final states characterized by the presence of a pair of leptons, quarks, and neutrinos are chosen for the signal. After the event selection, the precision of σ_{ZH}·Br(H→ZZ) is estimated to be 9.68%.

Keywords First keyword · Second keyword · More

1 Introduction

After the discovery of the Higgs boson [1,2], efforts are performed on measureing properties of the Higgs boson. One of motivations of these studies is to obtain hints for physics beyond the Standard Model (SM), whose existence is suggested by several experiment facts, such as dark matter, cosmological baryon-antibaryon asymmetry. The Circular Electron-Positron Collider (CEPC) [3, 4] is a proposed future circular e^+e^- collider, having its main ring circumstance of ∼100 km. As a Higgs factory, the CEPC is planned to operate at $\sqrt{s} = 240$ GeV with the integrated luminosity of $5.6ab^{-1}$ which is expected to achieve an order of magniutude improvement on measuremernts of Higgs boson properties as compared to the final LHC precision.

The Higgs production mechanisms at $\sqrt{s} = 240$ GeV will be the Higgsstrahlung process e^+e^-→Z*→ZH (hereafter, denoted as ZH process) and the vector boson fusion processes, $e^+e^- \to W^{+*}W^{-*}\nu_e\bar{\nu}_e \to H\nu_e\bar{\nu}_e$ ($\nu\bar{\nu}$H process) and $e^+e^- \to Z^*Z^*e^+e^- \to He^+e^-$, where the former is dominating over all of the others, therefore, is going to provide series of the Higgs measurements, such as the cross section $\sigma(ZH)$, using the recoil mass method against the Z boson. That Z boson also serves as a tag of the ZH process by identifying decay fermions from it. With this tag information, indivisual decay channels of the Higgs boson will be explored subsequently and give us valuable information on the Higgs boson properties ever.

The Higgs decay into a pair of Z bosons, via the ZH process, will be studied at the CEPC. Like the other decay modes, the Branching ratio BR(H→ZZ) can be obtained from the measurement of the signal yield, $\sigma(ZH)$×BR(H→ZZ). In addition, the Higgs boson width $\Gamma_{\rm H}$ can be inferred as well. Under the assumption that the coupling structure follows to that of the SM, the branching ratio is proportional to the term, BR(H→ZZ) = $\Gamma(\rm H\to ZZ)/\Gamma_{\rm H} \propto g^2_{\rm HZZ}/\Gamma_{\rm H}$, therefore, $\Gamma_{\rm H}$ is deduced with the uncertainty coming from the coupling $g^2_{\rm HZZ}$ ($\sigma(\rm ZH)\propto g^2_{\rm HZZ}$) and the signal yield. Note that the vector boson fusion $\nu\bar{\nu}$H process in combination with measurements of final states from H→WW decay will also give the $\Gamma_{\rm H}$ value and consequently the final value will be determined from both measurements[4, 5].

The study of H→ZZ channel via the ZH process has an unique feature among the other decays that is originated from its event toplogy where two on-shell Z bosons and one off-shell Z boson are involved. Considering various Z boson's decay possibilities, the topology diverges into lots of final states. H→ZZ→4l decay is the so-called "golden channel" of the Higgs boson study at the LHC, as it has the cleanest signature of all the possible Higgs boson decay modes, however, the small statistics of this leptonic channel at the CEPC may not

[a]e-mail: schsu@uw.edu
[b]e-mail: shixin@ihep.ac.cn

allow to study the properties with required precision. Conversely, fully hadronic channel can provide enough statistics, but difficulties in identifying and matching jets with proper Z bosons, as well as efficient separation from the SM backgrounds have to be overcome. Between these two extremes, the decay channles having a pair of leptons, jets and neutrinos are promising candidates for studying H→ZZ properties, owing to its clear signature and larger branching fraction than the leptonic channel. Therefore, this final state has been chosen as the signal for the evaluation of the HZZ properties. Muons have most advantage among charged leptons for discriminating isolated status from those produced by semi-leptonic decays of heavy flavor jets and the final states including a pair of muons are selected as the signal process: $Z \to \mu^+\mu^-$, $H \to ZZ^* \to \nu\bar{\nu}q\bar{q}$ (Fig. 1) and its cyclic permutations, $Z \to \nu\bar{\nu}$, $H \to ZZ^* \to q\bar{q}\mu^+\mu^-$ and $Z \to q\bar{q}$, $H \to ZZ^* \to \mu^+\mu^-\nu\bar{\nu}$, where the q represents all quark flavors except for the top quark.

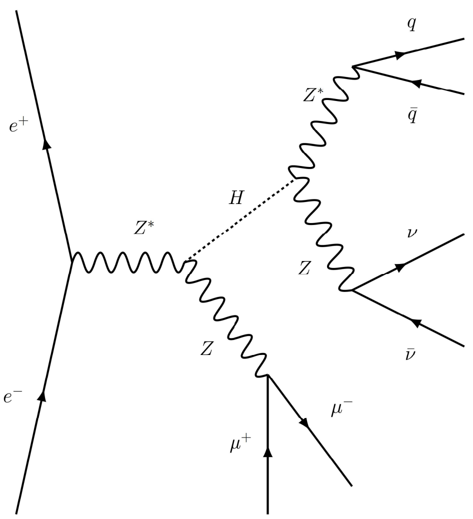

Fig. 1 Example feyman diagram of the signal process which is characterized by the presence of a pair of muons, jets and neutrinos. In this example, the initial Z boson associated with the Higgs production is decaying into muons whereas cyclic permutation of the decay products from 3 Z bosons is considered in the analysis.

In this article, we report on the estimation of relative accuracy of the yield measurement for the H→ZZ decay at the CEPC using the signal process characterized by the presence of a pair of muons, jets and neutrinos. In Section 2, we briefly introduce the CEPC detector design and the Monte Carlo (MC) simulation scheme. The event selection is described in Sec. 3, followed by an estimation on the precision of the signal yield in Sec. 4. Finally, conclusions are given in Sec. 5.

2 Detector design and simulation samples

The CEPC will hosts two interaction points (IP) on the main ring, where the detectors at each IP should record collision data under different center of mass energies varying from $\sqrt{s} = 91.2$ GeV as a Z factory to $\sqrt{s} = 240$ GeV as a Higgs factory. To fulfill those physics programs, a baseline concept is developed that is based on the ILC concept [6] with further optimizations for the CEPC environment. List it from the most inner subdetector component, the detector concept is composed of a silicon vertex detector, a silicon inner tracker consisting of micro strip detectors, a Time Projection Chamber (TPC), a silicon external tracker, ultra-fine segmented calorimeters, an Electronmagnetic CALorimeter (ECAL) and an Hadronic CALorimeter (HCAL), a 3T superconducting solenoid, and a muon detector [4].

The CEPC simulation software package implements the baseline concept detector geometry. Events for the SM processes are generated by the Whizard [7] including the Higgs boson signal, where the detector configuration and response is handled by the GEANT4-based simulation framework, MokkaPlus [8]. Modules for digitization of the signals at each sub detector creates the hit information. Particle reconstruction has been taken place with the Arbor algorithm, which builds the reconstructed particles using calorimeter and track information[9].

The Higgs boson production and decay are simulated with the scheme, where the generated sameples also contain the WW/ZZ fusion processes. All of the SM background samples, which can be classified into 2-fermion processes ($e^+e^- \to f\bar{f}$) and 4-fermion processes ($e^+e^- \to f\bar{f}f\bar{f}$), are produced as well.

3 Event Selection

Event selection is performed in several stages. The preselection builds higher-level objects, such as isolated muons, jets, and missing momentum from the Particle Flow (PF) objects which are reconstructed by the ArborPFA. The isolation requirements on muons, identified by the PFs, are imposed. For muons with energy higher than 3 GeV, tracks inside of a cone with a half-opening angle θ around the candidate are examined and it is identified as an isoloated muon, when a ratio between the energy of the muon candidate and a sumation of the energy from all of the tracks except for the candidate in a volume defined by the cone is higher than 0.1 with $\cos\theta = 0.98$. Jets are clustered from the PFs but except for isolated lepton candidates, using the k_t algorithm for the e^+e^- collision ($ee - kt$) with the FastJet package. Exclusive requirement ($N_{jet} = 2$) on number of jets is imposed. Events are requested to have a pair of isolated muons of positive and negative charged, and two jets successfully clustered.

The events satisfying the pre-selection criteria are separated into two categories separately for each of 3 final states in the signal process, according to the order of the invariant mass from di-objects which are not forming the tag of the initial Z boson. This categorization, distinguishing between the status having a pair of objects suppose to be decaying from the on-shell Z boson and that from the off-shell Z boson where H→ZZ* decay is assumed, enhances the efficiency of the event selection by appliying different selection criteria for each category respectively. Following notation is adopted for each category: $\mu\mu$H$\nu\nu qq$ is defined for the events with the reconstructed invariant mass of missing term $M_{\rm miss.}$ due to escaping neutrinos is larger than that of dijet $M_{\rm jj}$, where two characters of the top represent a pair of muons decaying from the initial Z boson.

On total 6 exclusive categories ($\mu\mu$H$\nu\nu qq$, $\mu\mu$H$qq\nu\nu$, $\nu\nu$H$\mu\mu qq$, $\nu\nu$H$qq\mu\mu$, qqH$\nu\nu\mu\mu$, qqH$\mu\mu\nu\nu$) the signal to background ratio is minimized by following requirements. The invariant mass $M_{\mu\mu}$ of the two muons, the invariant mass $M_{\rm jj}$ of two jets and the missing mass $M_{\rm miss.}$ are required to fall into the mass window around the Z(Z*) boson. Number of particle flow objects $N_{\rm PFO}$ in the event is required to be larger than a thoreshold value, which is affected and decided by the condition whether jets are originated from an on-shell Z boson or not, as well as to supress backgrounds where the jets are reconstructed from any objects other than quark seeds coming from the Z boson. Cut on the polar angle of the sum of all visible particles $\cos\theta_{\rm vis.}$ is applied to further reject background processes, such as two-fermion components which tends to be back-to-back along the z axis. To reduce contamination of signal events belong to the other category, further requirement on recoil mass distribuion is imposed at the final stage. Table **??** summarises the selection criteria applied across all the categories considered.

The signal and background reduction efficiencies and expected number of events running at $\sqrt{s} = 240$ GeV with an integrated luminosities of 5.6 ab^{-1} after the event selection is listed in the Table 2. In general, the analysis achieves a strong background rejection, while the signal selection efficiencies of approximately 30% and higher are kept. The main background which is common in all categories is the other Higgs decays. Four fermion processes, such as $e^+e^-\to$ZZ $\to\mu\mu qq$ and $e^+e^-\to$ZZ $\to\tau\tau qq$ due to the similarity of kinematics, have large contributions in the qqH$\mu\mu\nu\nu$ category and in the qqH$\nu\nu\mu\mu$ category, respectively.

4 Result

Precision of the yield measurement of $\sigma_{ZH}\times$Br(H→ZZ) is estimated. The obtained signal and background distributions for recoil mass spectrum against the initial Z boson in the range 110-140 GeV, are added to make up a pseudo-experimental result, while the Probablitlity Density Function (PDF) of both of the signal and the background are constructed indivisually by assuming the double-sided crystallball distribution for the Higgs decays including the signals and the Gaussian for the SM processes. Note that the background is made of the Higgs decays except for the signal and the SM processes The likelihood function is built from the the result as a observed events and PDFs as the number of expected events with the branching fraction Br(H→ZZ only for the signal component being a free parameter and the maximum likelihood fitting is performed. A detail description can be found in Ref. [5]. The recoil mass distribution together with the fitting curves is shown in Fig. 2.

Table 3 summarizes the derived relative precision $\Delta(\sigma\cdot{\rm BR})/(\sigma\cdot{\rm BR})$, where the bottom row shows the combined precision that is caluculated from the standard error of the weighted mean, $\sigma = 1/\sqrt{\sum_{i=1}^{n}\sigma_i^{-2}}$, where σ_i is the uncertainty for each category. The systematic uncertainty is not taken into account in this result. Estimates of relatice systematic uncertainty regarding to the precision measurement of σ_{ZH} at the CEPC is described in Ref. [10] and that's would be a base for the future study of the systematic uncertainty. The final result for the relative statistical uncertainty of the $\sigma_{ZH}\times$Br(H→ZZ) is estimated to be 9.68%.

5 Summary

The precision of the yield measurement $\sigma_{ZH}\times$Br(H→ZZ) at the CEPC is evaluated using MC samples for the baseline concept running at $\sqrt{s} = 240$ GeV with an integrated luminosities of 5.6 ab^{-1}. Among the various decay modes of the H→ZZ, the signal process having two muons, two jets and missing momentum in final states has been chosen. After the event selection, relative precision is evaluated with the lilehood fitting method on signal and background. The final value combined from all of six caterogies is estimated to be 9.68%.

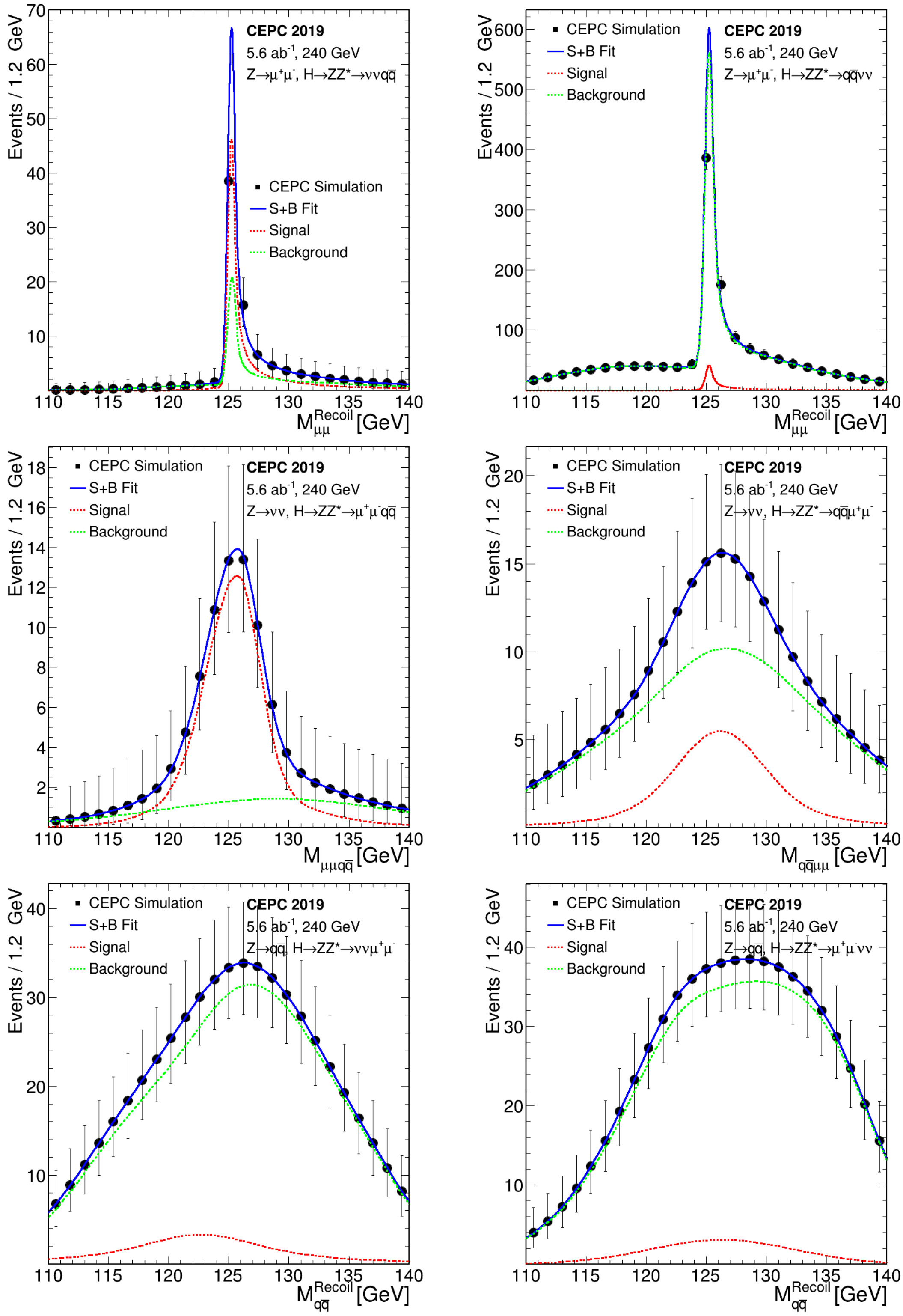

Fig. 2 Recoil mass distributions for each category. The black dots represent the predicted results at the CEPC and the solid blue line shows the fitting curve which is broken down into signal (dashed red line) and background (dashed green line) components.

Table 1 Overview of the requirements applied when selecting events.

Pre-selections						
$N(l) = 2$, where leptons(l) should pass the isolation criteria $N(\mu^+) = 1$, $N(\mu^-) = 1$ with $E(\mu^\pm) > 3$ GeV $N(jet) = 2$						
Variable	$\mu\mu\mathrm{H}\nu\nu qq$	$\nu\nu\mathrm{H}\mu\mu qq$	$\nu\nu\mathrm{H}qq\mu\mu$	$qq\mathrm{H}\nu\nu\mu\mu$	$qq\mathrm{H}\mu\mu\nu\nu$	$\mu\mu\mathrm{H}qq\nu\nu$
$M_{\mu\mu}$ (GeV)	[80, 100]	[60, 100]	[10, 60]	[15, 55]	[75, 100]	[80, 100]
M_{jj} (GeV)	[15, 60]	[10, 55]	[60, 100]	[75, 105]	[75, 110]	[60, 105]
$M_{\mathrm{miss.}}$ (GeV)	[75, 105]	[75, 110]	[75, 110]	[70, 110]	[10, 50]	[10, 55]
$M_{\mu\mu}^{\mathrm{recoil}}$ (GeV)	[110, 140]	-	[165, 215]	[175, 215]	[115, 155]	[110, 140]
$M_{\mathrm{vis.}}$ (GeV)	-	[110, 140]	[110, 140]	[115, 155]	[185, 215]	[175, 215]
$M_{\mathrm{jj}}^{\mathrm{recoil}}$ (GeV)	[185, 220]	-	-	[110, 140]	[110, 140]	-
N_{PFO}	[20, 90]	[20, 60]	[30, 100]	[40, 95]	[35, 100]	[30, 100]
$\lvert\cos\theta_{\mathrm{vis.}}\rvert$	< 0.95					
$\Delta\phi_{\mathrm{ZZ}}$ (degree)	[60, 170]	< 135	< 130	-	[120, 170]	[120, 170]
$\lvert M_{\mathrm{vis.}} - M_{\mathrm{H}}\rvert$ (GeV)	> 3	-	-	> 3	-	-
$\left\lvert M_{\mathrm{jj}}^{\mathrm{recoil}} - M_{\mathrm{H}}\right\rvert$ (GeV)	-	-	> 3	-	-	> 3
$\left\lvert M_{\mu\mu}^{\mathrm{recoil}} - M_{\mathrm{H}}\right\rvert$ (GeV)	-	> 3	-	-	> 3	-

Table 2 Summary of event selection.

	$\mu\mu\mathrm{H}\nu\nu qq$		$\nu\nu\mathrm{H}\mu\mu qq$		$\nu\nu\mathrm{H}qq\mu\mu$	
Process	ϵ [%]	$\mathrm{N}_{evt.}$	ϵ [%]	$\mathrm{N}_{evt.}$	ϵ [%]	$\mathrm{N}_{evt.}$
Signal	36	50	51	72	36	50
Higgs decays Bg.	$3.2{\cdot}10^{-3}$	36	$1.5{\cdot}10^{-3}$	17	$1.1{\cdot}10^{-2}$	130
SM four-fermion Bg.	$3.7{\cdot}10^{-6}$	4	$8.4{\cdot}10^{-6}$	9	$4.0{\cdot}10^{-5}$	43
SM two-fermion Bg.	$< 1.2{\cdot}10^{-7}$	0	$< 1.2{\cdot}10^{-7}$	0	$< 1.2{\cdot}10^{-7}$	0
	$qq\mathrm{H}\nu\nu\mu\mu$		$qq\mathrm{H}\mu\mu\nu\nu$		$\mu\mu\mathrm{H}qq\nu\nu$	
Process	ϵ [%]	$\mathrm{N}_{evt.}$	ϵ [%]	$\mathrm{N}_{evt.}$	ϵ [%]	$\mathrm{N}_{evt.}$
Signal	29	41	28	39	33	46
Higgs decays Bg.	$2.9{\cdot}10^{-2}$	326	$2.4{\cdot}10^{-2}$	275	$6.5{\cdot}10^{-2}$	738
SM four-fermion Bg.	$1.8{\cdot}10^{-4}$	190	$3.2{\cdot}10^{-4}$	345	$6.0{\cdot}10^{-4}$	644
SM two-fermion Bg.	$< 1.2{\cdot}10^{-7}$	0	$< 1.2{\cdot}10^{-7}$	0	$< 1.2{\cdot}10^{-7}$	0

Table 3 Statistical uncertainties on the product of the ZH cross section and the branching ratio. The bottom row shows the result of combined value of the 6 categories.

Channel		$\frac{\Delta(\sigma\cdot BR)}{(\sigma\cdot BR)}$ [%]
$Z\to\mu^+\mu^-$	$H\to ZZ^*\to\nu\bar{\nu}q\bar{q}$	18.1
$Z\to\mu^+\mu^-$	$H\to ZZ^*\to q\bar{q}\nu\bar{\nu}$	65.2
$Z\to\nu\bar{\nu}$	$H\to ZZ^*\to\mu^+\mu^- q\bar{q}$	13.5
$Z\to\nu\bar{\nu}$	$H\to ZZ^*\to q\bar{q}\mu^+\mu^-$	27.8
$Z\to q\bar{q}$	$H\to ZZ^*\to\mu^+\mu^-\nu\bar{\nu}$	63.9
$Z\to q\bar{q}$	$H\to ZZ^*\to\nu\bar{\nu}\mu^+\mu^-$	54.3
Combined		9.68

Acknowledgements

References

1. ATLAS Collaboration, G. Ada *et al.*, Observation of a new particle in the search for the Standard Model Higgs boson with the ATLAS detector at the LHC, Phys. Lett. B, **716**, 1-29 (2012), arXiv:1207.7214 [hep-ex]
2. CMS Collaboration, S. Chatrchyan *et al.*, Observation of a new boson at a mass of 125 GeV with the CMS experiment at the LHC, Phys. Lett. B, **716**, 30-61 (2012), arXiv:1207.7235 [hep-ex]
3. The CEPC Study Group, CEPC Conceptual Design Report: Volume 1 - Accelerator (2018), arXiv:1809.00285 [physics.acc-ph]
4. The CEPC Study Group, CEPC Conceptual Design Report: Volume 2 - Physics & Detector (2018), arXiv:1811.10545 [hep-ex]
5. F. An *et al.*, Precision Higgs physics at the CEPC, Chinese Physics C **43** no.4 (2019) 043002
6. T. Behnke *et al.*, The International Linear Collider Technical Design Report - Volume 4: Detectors (2013), arXiv:1306.6329 [physics.ins-det]
7. W. Kilian, T. Ohl, and J. Reuter, WHIZARD simulating multi-particle processes at LHC and ILC, Eur. Phys. J. C **71**, 1742 (2011), arXiv:0708.4233 [hep-ph]
8. P. Mora de Freitas and H. Videau, Detector simulation with MOKKA/GEANT4: Present and future, Presented at the International Workshop on Linear Colliders (LCWS 2002), 623-627 (2002), https://inspirehep.net/literature/609687
9. M. Ruan *et al.*, Reconstruction of physics objects at the Circular Electron Positron Colluder with Arbor, Eur. Phys. J. C **78** 426 (2018)

10. Z. Chen *et al.*, Cross section and Higgs mass measurement with Higgsstrahlung at the CEPC, Chinese Physics C **41** no.2 (2017) 023003